JOC The Journal of Organic Chemistry

Article

pubs.acs.org/joc

Reversible Photocapture of a [2]Rotaxane Harnessing a Barbiturate Template

Arnaud Tron,[†] Peter J. Thornton,[‡] Christophe Lincheneau,[†] Jean-Pierre Desvergne,[†] Neil Spencer,[‡] James H. R. Tucker,*[,‡] and Nathan D. McClenaghan*[,†]

[†]Institut des Sciences Moléculaires, CNRS UMR 5255, Université de Bordeaux, 33405 Talence, France

[‡]School of Chemistry, University of Birmingham, Edgbaston, B15 2TT Birmingham, United Kingdom

Supporting Information

ABSTRACT: Photoirradiation of a hydrogen-bonded molecular complex comprising acyclic components, namely, a stoppered thread (**1**) with a central barbiturate motif and an optimized doubly anthracene-terminated acyclic Hamilton-like receptor (**2b**), leads to an interlocked architecture, which was isolated and fully characterized. The sole isolated interlocked photoproduct (Φ = 0.06) is a [2]rotaxane, with the dimerized anthracenes assuming a head-to-tail geometry, as evidenced by NMR spectroscopy and consistent with molecular modeling (PM6). A different behavior was observed on irradiating homologous molecular complexes **1⊂2a**, **1⊂2b**, and **1⊂2c**, where the spacers of **2a**, **2b**, and **2c** incorporated 3, 6, and 9 methylene units, respectively. While no evidence of interlocked structure formation was observed following irradiation of **1⊂2a**, a kinetically labile rotaxane was obtained on irradiating the complex **1⊂2c**, and ring slippage was revealed. A more stable [2]rotaxane was formed on irradiating **1⊂2b**, whose capture is found to be fully reversible upon heating, thereby resetting the system, with some fatigue (38%) after four irradiation−thermal reversion cycles.

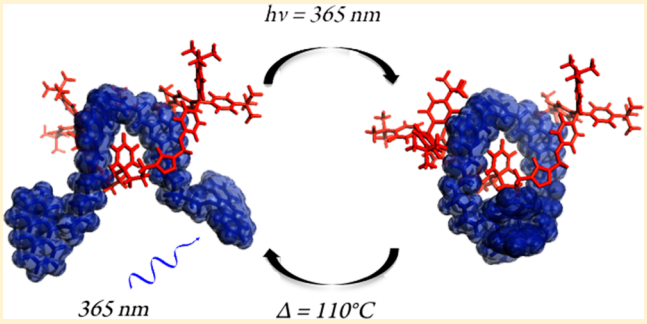

INTRODUCTION

Generation of mechanically interlocked molecules typically relies on preorganization or templating using self-assembly, notably harnessing noncovalent interactions between a molecular guest thread and a macrocyclic host, before covalent capture of the dynamic interpenetrating ensemble.[1] Ring-closing reactions often rely on reactions such as catalyzed ring-closing metathesis[2] or 1,3-dipolar cycloaddition/"click" reactions.[3] Photochemical versions are rather rare,[4] and reversible photocontrolled examples based on small molecules are, to the best of our knowledge, unknown. Considering two recently described examples of photochemical ring closure, Fujita reported one-way catenation of a Pt(II)-linked coordination ring induced by the photolabilization of a metal−pyridine bond.[4a] Li and Li described an organic system where macrocyclization was achieved through an irreversible photochemical example based on a thiol−yne click reaction under UV irradiation.[4b,c]

Here we report the formation of a hydrogen-bonded complex between a stoppered molecular thread (**1**) with a central barbiturate and a photoactive acyclic Hamilton-type receptor (**2**) and subsequent light-driven ring closure to form the [2]rotaxane with thermal reopening to reset the system. The ensemble of processes is summarized in Figure 1, while structural formulas of the investigated target molecules are shown in Scheme 1. The photoactive receptor (**2**) comprises two terminal 9-alkoxyanthracene units, which upon photoirradiation permit closure of the cycle around an enveloped guest via a photodimerization reaction. The size of the cycle plays a determinant role with respect to generation of a kinetically inert interlocked structure, as evidenced by the photoproducts of **2a**, **2b**, and **2c** in the presence of thread **1** (*vide infra*). While anthracene photodimerization has previously been reported by us and others to afford classic supramolecular structures such as crown ethers and cryptands,[5,6] this is the first example of its use in the formation of an interlocked structure from acyclic components, and more precisely a [2]rotaxane. Interestingly, anthracene photodimerization has been shown to control threading−dethreading rates of noninterlocked pseudorotaxanes by adjusting macrocycle ring size,[7] as well as to interconvert a poly(rotaxane) into a mixture of oligomeric, polymeric, and cyclic photoproducts.[8] Recently, we described a copper-catalyzed, nonphotochemical barbiturate-templated rotaxane formation via hydrogen-bonded preorganization between a barbiturate thread and a cyclic Hamilton receptor, followed by the "click" stoppering reaction.[9] Fidelity between partners is assured by an array of six complementary hydrogen bonds, orienting the bead and thread in an orthogonal arrangement, evidenced by X-ray crystallographic data.[9] Introduction of photoactive groups now allows light-driven rotaxane assembly using a barbiturate-templating

Received: November 1, 2014
Published: December 5, 2014

   dx.doi.org/10.1021/jo502452t | J. Org. Chem. 2015, 80, 988−996

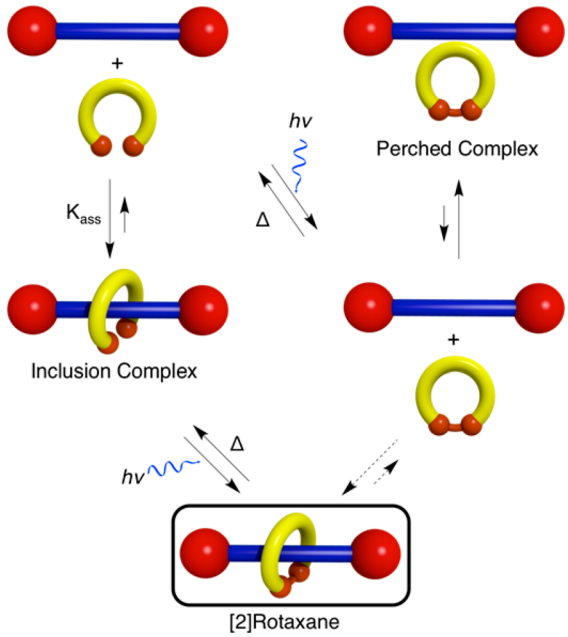

Figure 1. Schematic representation of [2]rotaxane formation by photoclipping an acyclic receptor bearing terminal anthracene groups onto a stoppered thread and disassembly by thermal retrocyclomerization. Slippage in the case of a large ring is also represented.

motif. This prototype system was designed to allow both investigation of a templated photochemical macrocyclization reaction, as well as the reversible generation of an interlocked [2]rotaxane structure. Orthogonality of photochemical transformations with regard to other chemical processes could potentially allow incorporation into multicomponent stimulus-responsive molecular machines.

Variants of receptor **2**, previously synthesized in the Tucker group, were employed in the context of modulating barbiturate binding affinity when small cycles (30 members) were employed.[10] Here larger variants were developed and harnessed to ensure comfortable barbiturate encapsulation on the thread **1**, while the upper size limit of the desired ring is determined by thermal slippage efficiency over the trityl stopper groups. Investigation of **2a**, **2b**, and **2c**, whose ring-closed variants ($\mathbf{2a_C}$, $\mathbf{2b_C}$, and $\mathbf{2c_C}$, respectively) represent cycles with 30, 36, and 42 members, served to elucidate the optimal size of the photoactive molecular component.

RESULTS AND DISCUSSION

Molecular Modeling and Design. The structural formulas of the target molecules are shown in Scheme 1. Molecular thread **1** was used throughout the study as a guest for the Hamilton receptor-containing photoactive receptor **2**. Molecule **1** comprises a central barbiturate motif, whose central sp^3 carbon assures an orthogonality of the substituents with respect to the barbiturate plane, which was anticipated to afford enhanced binding of **2** in supramolecular **1⊂2**.[9] Trityl stopper groups incorporating three *tert*-butyl groups were employed to confer kinetic inertness to the closed [2]rotaxane structure $\mathbf{1{\subset}2_C}$. Scheme 1 further illustrates an idealized overview of the formation of supramolecular host–guest complex **1⊂2**, photochemical capture of the [2]rotaxane structure $\mathbf{1{\subset}2_C}$, and subsequent thermal reversion to the initial complex. In practice, the thermal stability of the interlocked structure would depend on the type of anthracene photodimer generated, be it a stable

Scheme 1. Structures of 1, 2a, 2b, and 2c, Assembly of Molecular Complex 1⊂2, Photogeneration of a [2]Rotaxane of type $\mathbf{1{\subset}2_C}$, and Subsequent Thermal Reversion

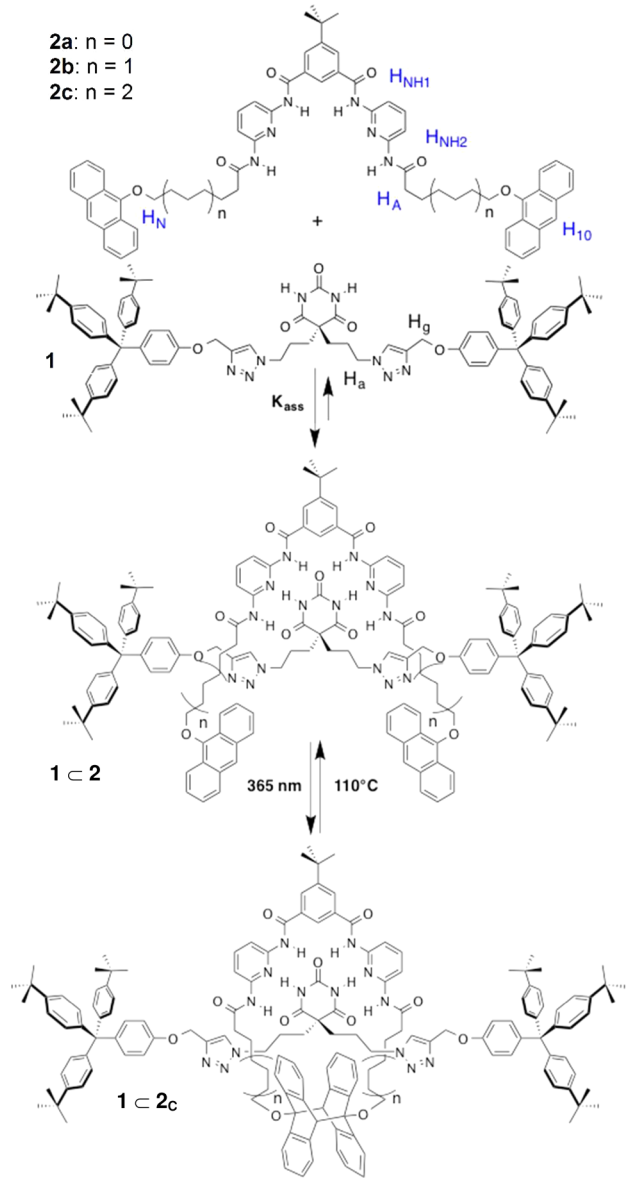

antiparallel so-called "head-to-tail" (HT) photodimer (represented in Scheme 1) or the transient head-to-head (HH) photodimer (not shown). This assumes a likely [4π + 4π] cyclomerization reaction involving the central anthracene cycles, although other variants are known.[11] The distribution of HH and HT photoproducts and efficiency of the photoreaction may in turn be partly governed by the dynamic/conformational properties of the flexible chains in the receptor, and flexibility is anticipated to be highest for **2c** and lowest for **2a**. Equally, kinetic stability for systems with larger bead rings demands negligible slippage over stopper groups, so a compromise between conformational flexibility and kinetic stability is required in the case of interlocked $\mathbf{1{\subset}2_C}$.

The subtle combination of these different parameters on the outcome of the photochemical reactions, along with product stability, precludes absolute certainty in prediction of performance. Nevertheless, molecular modeling was employed to give credence to the design of molecular components and

dx.doi.org/10.1021/jo502452t | J. Org. Chem. 2015, 80, 988–996

assemblies. Calculated molecular structures (see Figure 2 and Supporting Information) considering van der Waals surfaces

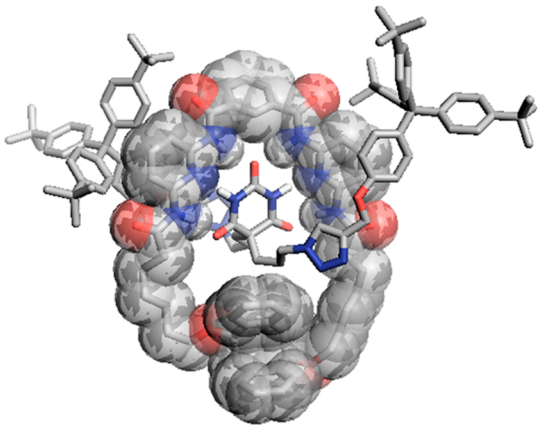

Figure 2. Calculated structure of [2]rotaxane **1⊂2b**$_C$ (PM6 minimization). Hydrogen atoms that are not implicated in hydrogen bond formation are omitted for clarity.

afford an estimation of the size of the substituted trityl group at ca. 88 Å^2, as well as the maximal macrocycle ring void sizes of **2a**$_C$, **2b**$_C$, and **2a**$_C$ at 43, 68, and 110 Å^2, respectively.

The calculated structure of rotaxane **1⊂2b**$_C$, with an intermediate bead ring size (PM6 minimization), is shown in Figure 2. It nicely supports the interpenetrating nature of the thread **1**−macrocycle **2b** photoproduct and the existence of strong interactions between them, despite the bulky "butterfly"-like geometry of the anthracene photodimer. The short contact interactions are ascribed to six complementary hydrogen bonds between the two entities of the [2]rotaxane (DADDAD and ADAADA for receptor and guest, respectively), whose bond lengths [N−H···O═C] (anticlockwise from left to right, Figure 2) are 1.9, 2.0, 2.1, 2.1, 2.0, and 1.9 Å with angles of 153° to 172°. The similarity in the values implies a symmetric, stable system. While the calculated van der Waals surface of this [2]rotaxane shows an adapted cavity for the complexation of the barbiturate motif and for the proposed interlocked structure comprising macrocyle **2b**$_C$ and thread **1**, the homologous structures formed with **2a** (Figure S2, Supporting Information) and **2c** (Figure S3, Supporting Information) appear somewhat different. Complex **1⊂2a**$_C$ appears unfavorable due to the restricted ring size, which may favor HH photodimer formation. Complex **1⊂2c**$_C$ shows a substantial cavity size due to the incorporation of six additional methylene groups with respect to **1⊂2b**$_C$, and the high degree of flexibility may be anticipated to have consequences with respect to ring slippage (*vide infra*) and possibly kinetics of translation in future multistation assemblies comprising these motifs.

Synthesis. The synthesis of receptors **2a** and **2b**[10] and barbiturate thread **1**[9] was described previously. All new compounds were fully characterized by ^{1}H and ^{13}C NMR spectroscopies (Figures S37, S38, S39, S40, S41, S42, S43, and S44, Supporting Information) and by mass spectrometry, in particular the [2]rotaxane **1⊂2b**$_C$ (Figure S1, S20, S33, and S36, Supporting Information). The formation of a new homologous receptor (**2c**) with a longer spacer was developed in analogy to the previously reported methodology, as outlined in Scheme 2, and was purified by column chromatography on silica (eluent dichloromethane/ethyl acetate, 8:2, v/v). For the preparation of photodimers **2**$_C$ (Scheme S1, Supporting

Scheme 2. Synthesis of Acyclic Receptor 2c

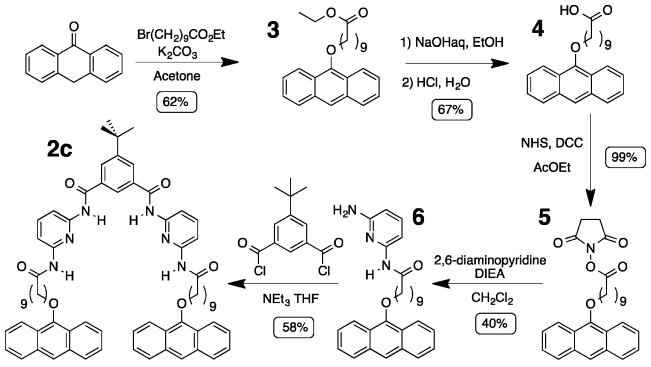

Information) from the anthracene-appended receptors **2**, preparative photoirradiation was performed. For a large scale preparation, a solution filter is used (lead nitrate/sodium bromide filter, 7 g·L^{-1}; KBr 540 g·L^{-1}), which cut UV light below 350 nm.[12] The light source was a Hanovia 450 W HgXe lamp. High dilution conditions (5×10^{-4} M) and degassed solvents were used to avoid photoinduced intermolecular processes and oxidation of the anthracene moieties. The reaction was followed by UV−vis spectroscopy on monitoring the disappearance of the lowest-energy anthracene absorption band (350−420 nm). Cyclized receptors **2a**$_C$, **2b**$_C$, and **2c**$_C$ were isolated by column chromatography (SiO_2, dichloromethane/ethyl acetate, 9:1, v/v) or by semipreparative HPLC (mobile phase, gradient 10% ethyl acetate/cyclohexane to 100% ethyl acetate in 50 min) with 36%, 42%, and 40% yield, respectively. Although the photodimerization of 9-substituted anthracenes can lead to the formation of head-to-head (HH) and head-to-tail (HT) photodimers, only HT photoproducts **2a**$_C$, **2b**$_C$, and **2c**$_C$ were isolated from the irradiated mixtures. This is partly due to the rapid thermal return of the population of the sterically encumbered HH photodimers, relative to the persistent, antiparallel HT dimers (*vide infra*).[11]

Having the inclusion complex **1⊂2b** in hand, photoinduced covalent capture of interlocked [2]rotaxane **1⊂2b**$_C$ could be performed. In order to maximize the production of the interlocked structure, generation of the initial supramolecular complex **1⊂2** was optimized by using a relatively high solute concentration (0.5 mM), while keeping possible intermolecular photoreactions to a minimum and augmenting the quantity of photoinert thread **1** (3 mol equiv) with respect to **2**. In the case of **2b**, this equated to an initial proportion of bound **1⊂2b** that was >97% in DCM. Following degassing by multiple freeze−pump−thaw cycles and subsequent irradiation, the [2]rotaxane **1⊂2b**$_C$ and free **2b**$_C$ were isolated by column chromatography (SiO_2, dichloromethane/ethyl acetate, 9:1, v/v) or by semi-preparative HPLC (mobile phase, gradient 10% ethyl acetate/cyclohexane to 100% ethyl acetate in 50 min) in 58% and 30% yield, respectively. As observed for free receptor **2b**, only the HT photoproduct, in this case, the [2]rotaxane **1⊂2b**$_C$ (Scheme S2, Supporting Information) was isolated from the irradiated **1⊂2b** mixture. The cyclized receptor **2b**$_C$ could also be obtained in a higher yield (42%) in the absence of **1**. Rotaxanes **1⊂2a**$_C$ or **1⊂2c**$_C$ were not isolated following column chromatography (*vide infra*), but rather individual thread **1** and closed receptor components **2a**$_C$ or **2c**$_C$ were obtained.

Binding Studies for 1⊂2. Formation of supramolecular complex **1⊂2** could be followed by ^{1}H NMR and UV−vis spectroscopy. Analysis of the complexation-induced red-shifting

dx.doi.org/10.1021/jo502452t | J. Org. Chem. 2015, 80, 988−996

of the pyridine absorption band of receptors **2a**, **2b**, and **2c** at 315 nm upon interaction with thread **1** allowed determination of the elevated binding constants in dichloromethane, which increased as a function of the length of the aliphatic receptor arms in the order **2a** < **2b** < **2c**. Values obtained for binding **1** by **2a**, **2b**, and **2c** were K_{ass} = 30 000 M^{-1} (Figure S4, Supporting Information), K_{ass} = 55 000 M^{-1} (Figure S5, Supporting Information), and K_{ass} = 65 000 M^{-1} (Figure S6, Supporting Information), respectively. Note that these high values precluded binding constant determination by NMR analysis. A 1:1 stoichiometry of the supramolecular inclusion complexes **1⊂2a/b/c** was confirmed via Job plots (Figure S7, Supporting Information), because the maximum absorbance change was obtained when the molar fraction ratio reached 0.5. Further evidence for the close proximity of the receptor **2** to the stoppered thread **1** was provided by fluorescence emission quenching of the acyclic receptor induced by the presence of **1**. The addition of thread resulted in a decrease of fluorescence intensity of the inclusion complexes **1⊂2a**, **1⊂2b**, and **1⊂2c** (Φ_f = 0.22, 0.13, and 0.20, respectively) compared with the free receptors (Φ_f = 0.33, 0.22, and 0.26 for **2a**, **2b**, and **2c**, respectively), presumably due to additional vibrational deexcitation or nonemissive complex formation. The fluorescence quantum yield determination method is described in Supporting Information.[13]

Hydrogen bonding in solution, leading to complex **1⊂2** was also evidenced by ^{1}H NMR spectroscopy (for example, see Figure 3b and Figure S9, Supporting Information, for receptor **2b**). The different chemical shift values (δ) of the N−H resonances and pertinent aliphatic protons (H_A of the receptor part, H_a and H_g of the barbiturate part) of the inclusion complex **1⊂2** and the uncomplexed constituents are summarized in Table 1. Addition of 1 equiv of guest to the acyclic receptor **2a/b/c** (10 mM, CD_2Cl_2, Figures S8, S9, and S10, Supporting Information) resulted in strong downfield shifts of the N−H resonances of the barbiturate ($\Delta\delta$ = 3.91, 3.63, and 3.56 ppm, respectively) and those of the amide protons of the receptor: $\Delta\delta$ = 1.18 and 1.23 ppm for **2a** (Figure S8, Supporting Information); 0.87 and 1.03 ppm for **2b** (Figure S9, Supporting Information); and 0.97 and 1.19 ppm for **2c** (Figure S10, Supporting Information), compared with uncomplexed barbiturate thread **1** and receptor **2**.

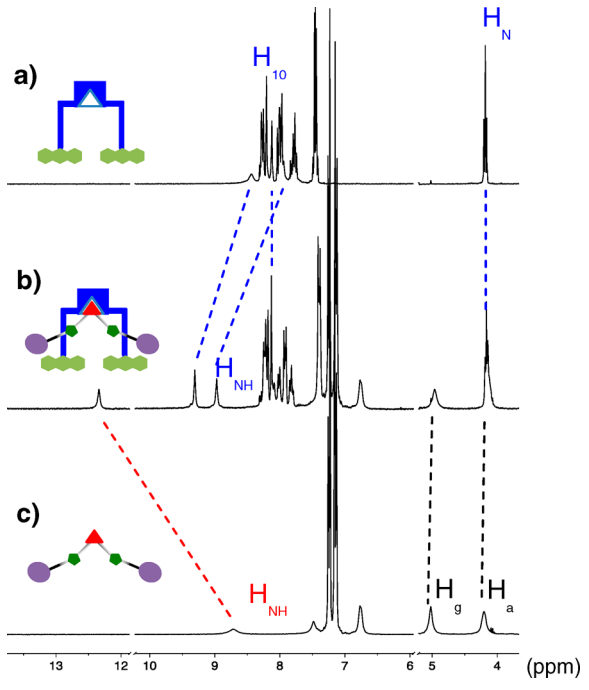

Figure 3. Partial ^{1}H NMR spectra (600 MHz) of acyclic receptor **2b** (a), complex **1⊂2b** (1:1, 10 mM) (b), and barbiturate thread **1** (c) recorded at room temperature in CD_2Cl_2. The assignments of protons refer to those indicated in Scheme 1.

Table 1. Chemical Shifts from ^{1}H NMR for the Supramolecular Complex 1⊂2 and the Uncomplexed Molecules 1 and 2 (300 MHz, CD_2Cl_2, 293 K)

	receptor protons			barbiturate protons		
compound/complex	H_{NH1}	H_{NH2}	H_A	H_{NH}	H_a	H_g
1				8.71	4.20	5.02
2a	8.41	8.02	2.85			
1⊂2a	9.59	9.25	2.84	12.62	3.73	4.86
2b	8.44	7.94	2.44			
1⊂2b	9.31	8.97	2.46	12.34	4.13	4.96
2c	8.38	7.68	2.39			
1⊂2c	9.35	8.87	2.40	12.27	4.24	5.02

NOESY NMR experiments on supramolecular complex **1⊂2b** evidenced the close proximity between amide protons of receptor **2b** and the imide protons of thread **1** (Figure S11, Supporting Information) and confirmed a weak interaction between the two species. Similarly, resonances corresponding to protons H_a of the two aliphatic arms of **1** correlated with the methylene protons H_A of the alkyl chain of receptor **2b**. These observations are consistent with the formation of a supramolecular complex predisposed to perform a photoclipping reaction of receptor **2b** onto stoppered thread **1** to give the [2]rotaxane.

Photodimerization and Thermal Reversion. Rotaxane formation via a process of photoclipping of receptor **2** onto barbiturate **1** in dichloromethane was followed by UV−vis and fluorescence spectroscopy. The characteristic structured near-UV absorption band of the anthracene chromophore and its disappearance upon photodimerization allowed studies of the evolution of the photoreaction as a function of the irradiation time. On irradiation of the complex **1⊂2b** at 365 nm in degassed CH_2Cl_2, the disappearance of anthracene absorption bands ascribed to the $S_1 \leftarrow S_0$ (330−400 nm) and $S_2 \leftarrow S_0$ (260 nm) transitions was observed (Figure 4). This is consistent with the photodimerization of the anthracene subunit and the acyclic receptor **2**, at a concentration of 25 μM, undergoing an intramolecular process leading to the cyclic receptor $\mathbf{2}_C$ (which was fully confirmed by the reaction quantum yields, which were found to be concentration independent, *vide infra*).

A similar conclusion can be drawn from fluorescence studies (Figure S14, S15, and S16, Supporting Information), since the photoreactions were conducted at very low concentration ($\leq 10^{-5}$ M), which is unfavorable for intermolecular cycloaddition. The characteristic structured emission band, with maxima at 400, 420, and 440 nm, of the anthracene units disappeared upon irradiation at 365 nm with a conversion of 93%, 78%, and 82% for the mixtures **1⊂2a**, **1⊂2b**, and **1⊂2c**, respectively, compared with the corresponding free receptor, whose photoconversion was 99%, 87%, and 94%, respectively. The decreasing fluorescence of receptor **2** paralleled the formation of the photodimer ($\mathbf{2}_C$). In the presence of barbiturate **1**, a similar process was observed, and the

dx.doi.org/10.1021/jo502452t | J. Org. Chem. 2015, 80, 988−996

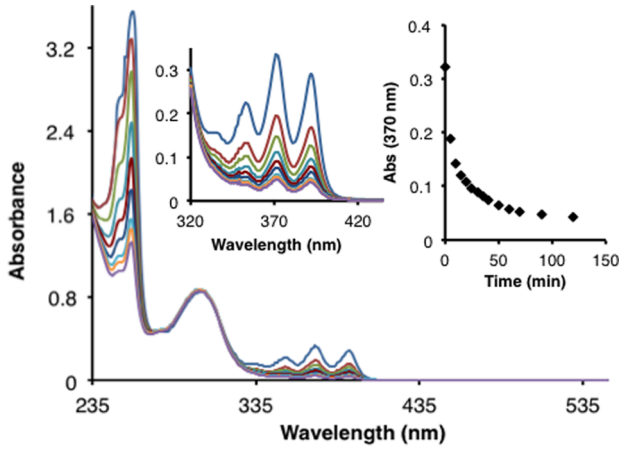

Figure 4. Absorption spectra of **1⊂2b** (25 μM, 1:1) in CH_2Cl_2. Upon irradiation at 365 nm, the disappearance of the anthracene moieties and hence absorption at 370 nm continued until 90% of the starting material was converted.

absorption spectra of the inclusion complexes **1⊂2** indicate the complexation between the two species.

Light-driven [2]rotaxane formation was anticipated by ring closure via dimerization of terminal anthracene groups of the appropriate receptor **2** around thread **1**. It should be noted that the photodimerization of 9-substituted anthracenes can lead to the formation of head-to-head (HH) and head-to-tail (HT) photodimers, which could potentially give rise to a small library of photoproducts. Only a single product appeared to be present after irradiation of the **1⊂2b** complex at 365 nm for 1 h, as judged by ^{1}H NMR analysis (described below). However, the concomitant formation of two different photodimers of **1⊂2b$_C$** (and **2b$_C$**, when the receptor was irradiated alone) was evidenced by observing changes to the anthracene absorption band upon sequential cycles of irradiation at 365 nm for a short time (180 s) followed by thermal reversion at 298 K. Immediately after irradiation, spontaneous return of the anthracene absorption band at 370 nm, with a retroconversion of 14% (for the first cycle) over a period of 2600 s was observed (Figure S17, Supporting Information). This relatively rapid change was attributed to the predominant retrodimerization of the HH photodimer, which is generally considered less stable,[11] while the substantially more stable species can be reasonably attributed to the HT photodimer. The observed rate constants of the room temperature retrodimerization (k_{retro})[5,14] of the HH photodimers to the starting complex **1⊂2b** (Figure S17, Supporting Information) and the free **2b** receptor (Figure S18, Supporting Information) were determined to be 2.8×10^{-4} and 7.5×10^{-4} s^{-1}, respectively, with corresponding half-lives of 25 and 14 min. This assumes a negligible retrodimerization of the HT photoproduct. These values are in agreement with those previously published for HH photodimers.[14] In the case of the HT photodimers of **1⊂2b$_C$** and free macrocycle **2b$_C$**, reversion back to the starting materials was possible by heating at an elevated temperature. Upon complete formation of the HT photodimers from the inclusion complex **1⊂2b** (or free receptor **2b**) after 1 h of irradiation at 365 nm, the retrodimerization was performed by heating the solution at 110 °C for 14 h, leading to a retroconversion of 81% (83% in the case of **2b$_C$**). A summary of these observations concerning the cycle of photocapture of [2]rotaxane **1⊂2b$_C$** as HH and HT photodimers from the inclusion complex complex **1⊂2b** and subsequent reconstitution is illustrated in Figure 5.

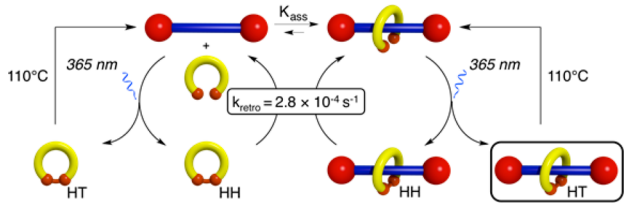

Figure 5. Schematic representation of kinetic and thermodynamic photoproducts formed from molecular thread **1** and receptor **2** and their interconversion.

Rotaxane formation and disassembly can thus be controlled via external stimuli. The reversibility of the process over multiple cycles was studied using a solution of **1⊂2b** (Figure 6),

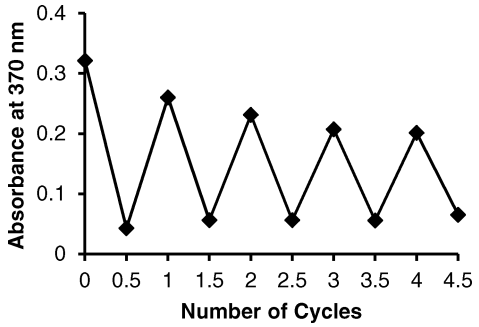

Figure 6. Fatigue study of a 25×10^{-6} M solution of supramolecular complex **1⊂2b** (40:1) in degassed CH_2Cl_2 monitored by UV−vis spectroscopy. Each cycle corresponds to irradiation at 365 nm (1 h), promoting photocyclization, followed by thermal retrodimerization (110 °C, 14 h).

by repeating a cycle of irradiation at 365 nm for 1 h, followed by thermal retrodimerization at 110 °C over 14 h. The percentage of photodimers (mixture of **1⊂2b$_C$** and free **2b$_C$**) after each closing process and the percentage of host−guest complex **1⊂2b** (as the high association ensures quasi-quantitative complexation) after each opening process was determined by monitoring changes to the absorption intensity at 370 nm. A fatigue study showed that more than 80% of the anthracene chromophore was recovered after each cycle (Figure 6), with a total fatigue of 38% after four cycles. Photochemical reversion on irradiation of the photodimers far into the UV (280 nm) resulted in a higher degree of fatigue or buildup of irreversible photoproducts.[11]

The quantum yield (Φ_r) of the photodimerization reactions was determined, affording a measure of the efficiency of the photoprocesses for the different systems (receptor **2a**/**b**/**c** in presence and in absence of **1**), as well as information on the nature of the intra- or intermolecular photodimerization. The quantum yield determination methods are described in the Supporting Information.[15] The intramolecular nature of the photodimerization was confirmed by the unchanging value of Φ_r = 0.06 for solutions of **1⊂2b** at three different concentrations: (i) 25×10^{-6} M, (ii) 5×10^{-5} M, and (iii) 5×10^{-4} M. Following a similar trend in the fluorescence emission data, the addition of thread **1** resulted in a decrease in the intramolecular photodimerization quantum yields (Φ_r) for the inclusion complexes **1⊂2a**, **1⊂2b**, and **1⊂2c** (Φ_r = 0.04,

dx.doi.org/10.1021/jo502452t | J. Org. Chem. 2015, 80, 988−996

0.06, and 0.10, respectively) compared with the corresponding free receptors (Φ_r = 0.07, 0.08, and 0.17, respectively).

^{1}H NMR Spectroscopic Characterization of [2]-Rotaxane 1⊂2b$_C$. The ^{1}H NMR spectrum of **1⊂2b$_C$** (Figure 7b) shows downfield shifts of several signals with respect to

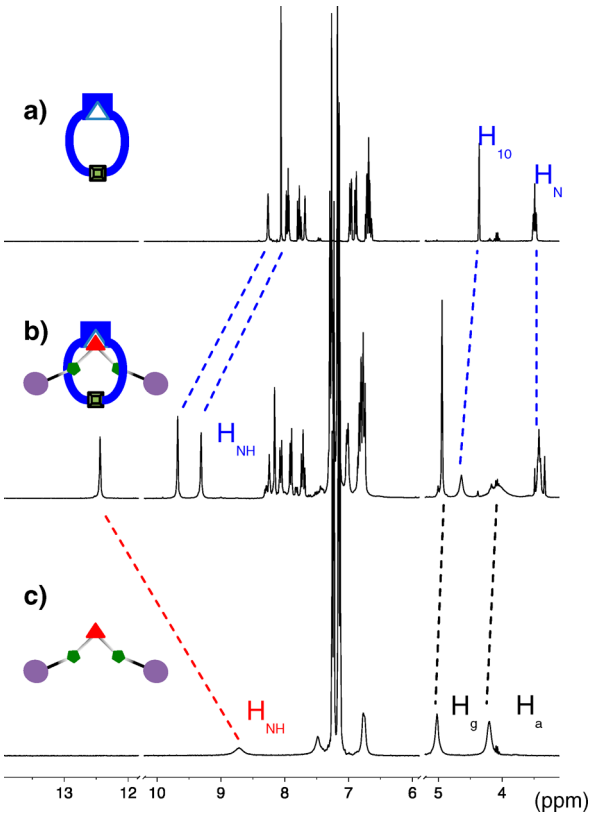

Figure 7. Partial ^{1}H NMR spectra (600 MHz) of macrocyclic receptor **2b$_C$** (a), [2]rotaxane **1⊂2b$_C$** (b), and barbiturate thread **1** (c) recorded at room temperature in CD_2Cl_2. The assignments of protons refer to those indicated in Scheme 1.

noninterlocked **2b$_C$** and **1** (Figure 7a,c, respectively). In particular, downfield shifts of the amide proton signals of the macrocycle ($\Delta\delta$ = 1.2 and 1.3 ppm) and those of the barbiturate protons in the thread ($\Delta\delta$ = 3.7 ppm) indicate H-bonding interactions. Stronger hydrogen bonding in **1⊂2b$_C$** compared with complex **1⊂2b** is inferred through further downfield shifting and sharpening of the barbiturate imide H_{NH} resonance ($\Delta\delta$ = 0.10 ppm; Figure 7b cf. Figure 3b) and those of the amide protons of the receptor ($\Delta\delta$ = 0.3 ppm). The interlocked nature of pure **1⊂2b$_C$** was also evidenced by DOSY NMR experiments (Figure S19, Supporting Information) allowing the determination of the diffusion rates of various species in the system. Indeed, in the case of inclusion complex **1⊂2b**, DOSY NMR spectra show different diffusion coefficients of barbiturate **1** (0.31×10^{-9} m^2 s^{-1}, Figure S19c, Supporting Information) and receptor **2b** (0.65×10^{-9} m^2 s^{-1}, Figure S19c, Supporting Information), whereas at the same concentration, [2]rotaxane **1⊂2b$_C$** (Figure S19d, Supporting Information) exhibited a common diffusion coefficient (0.38×10^{-9} m^2 s^{-1}) for both the barbiturate and the receptor parts. This is taken as evidence of the interlocked nature of the two components. ROESY NMR experiments on pure [2]rotaxane **1⊂2b$_C$** show a through-space correlation between amide protons of receptor **2b$_C$** and the imide protons of thread **1** (Figure S20, Supporting Information) and confirmed their close proximity in the complex. Similarly, resonances corresponding to protons H_a of the two aliphatic arms of **2** correlated with the methylene protons (most clearly visible with H_A) of the alkyl chain of the receptor part. These observations are consistent with the position of the two arms of the guest **1** embracing both sides of the macrocycle cavity, a prerequisite in an interlocked structure.

Moreover, ^{1}H NMR allowed the investigation of the photoclipping process giving rise to [2]rotaxane **1⊂2b$_C$**. Complete disappearance of the anthracene proton signals (δ = 7.90−7.95 and 7.48−7.42 ppm, in CD_2Cl_2) of the inclusion complex **1⊂2b** (Figure 3b) was observed and two multiplet signals assigned to the aromatic protons of the [2]rotaxane appeared at 7.00 and 6.80 ppm, after photocapture of the receptor **2b$_C$** on thread **1**. Another indication of this [2]rotaxane formation process was the appearance of a singlet at 4.64 ppm, which was attributed to the H_{10} aliphatic proton concomitant with the disappearance of the anthracene H_{10} aromatic proton at 8.16 ppm. The appearance of this singlet signal, corresponding to the bridgehead protons of the [2]rotaxane, confirms the occurrence of [4π + 4π] photocycloaddition between the central rings on each anthracene unit. Inspection of the aromatic resonances of the photodimer suggests a head-to-tail formation, similar to the photodimer **2$_C$** in the absence of thread **1**. The ^{13}C NMR spectra also provided confirmation of the [4π + 4π] photocycloaddition giving [2]rotaxane **1⊂2b$_C$** (Figure S21b, Supporting Information), due to the appearance of two aliphatic resonances: 89.5 ppm, which is assigned to the two new similar quaternary anthracene carbons (carbon directly connected to the alkoxy function) and 63.5 ppm, corresponding to the two sp^3-hybridized CH groups on the central ring (carbon directly connected to H_{10}), compared with those of complex **1⊂2b** (Figure S21a, Supporting Information) at 134.0 and 122.6 ppm, respectively.

Variable temperature ^{1}H NMR experiments were also performed in $CDCl_3$ (which has a higher boiling point than CD_2Cl_2) in order to assess the H-bonding interaction in the [2]rotaxane **1⊂2b$_C$** (Figure S23, Supporting Information, 5 mM). Upon cooling of the solution to 0 °C, a small downfield shift ($\Delta\delta$ = 0.11 ppm) of the imide proton resonances was observed, due to increased H-bonding. On heating of the solution to 55 °C an upfield shift ($\Delta\delta$ = 0.23 ppm) of the imide proton resonances was observed. In both cases, only a very small effect on the amide proton resonances was observed. Also, no dethreading was evidenced upon heating the solution to 55 °C.

Tests of Slippage and Analysis of Potential Perched Products. Further evidence for the interlocked nature of the complex **1⊂2b$_C$** comes from a comparison of ^{1}H NMR data of **1⊂2b$_C$** (Figure S22a, Supporting Information, 5 mM) with the noninterpenetrating, perched complex **1·2b$_C$** (Figure S22b, 1:1, 5 mM), formed by mixing thread **1** and the preformed receptor **2b$_C$** in CD_2Cl_2. In particular, differences for both barbiturate imide proton resonances ($\Delta\delta$ = 0.42 and 0.57 ppm) and the two signals of the amide protons of **2b$_C$** ($\Delta\delta$ = 0.75 ppm) were observed between interlocked and perched complexes under the same conditions. Perched complexes between **1** and the receptors **2a$_C$** and **2c$_C$** were also evidenced by ^{1}H NMR spectroscopy, although they behaved differently than the **2b$_C$** case. For perched complex **1·2a$_C$** (Figure S25b, Supporting Information, 1:1, 5 mM), an apparent upfield shift ($\Delta\delta$ = 1.27 ppm) of imide proton resonances compared with the unbound compound (Figure S25a and S25c, Supporting Information)

dx.doi.org/10.1021/jo502452t | J. Org. Chem. 2015, 80, 988−996

Table 2. Chemical Shift Values from ^{1}H NMR for the Supramolecular Complexes $\mathbf{1}\cdot\mathbf{2}_C$, Their Uncomplexed Constituents, and [2]Rotaxane $\mathbf{1}\subset\mathbf{2b}_C$ (300 MHz, 5 mM, CD_2Cl_2, 293 K)

	receptor part			barbiturate part		
compound/complex	H_{NH1}	H_{NH2}	H_A	H_{NH}	H_a	H_g
1				8.71	4.20	5.02
$\mathbf{2a}_C$	8.49	8.05	2.72			
$\mathbf{1}\cdot\mathbf{2a}_C$	8.52	8.05	2.72	7.54	4.25	5.09
$\mathbf{2b}_C$	8.16	7.60	2.41			
$\mathbf{1}\cdot\mathbf{2b}_C$	9.26	8.74	2.43	11.69	3.63	4.98
$\mathbf{1}\subset\mathbf{2b}_C$	9.68	9.31	2.38	12.44	4.08	4.94
$\mathbf{2c}_C$	8.33	7.67	2.37			
$\mathbf{1}\cdot\mathbf{2c}_C$	9.70, 8.97	9.23, 8.37	2.39	12.55, 10.13	3.55	4.95

was the only observation, due to the restricted ring size of the $\mathbf{2a}_C$. As for a mixture of **1** and largest macrocycle $\mathbf{2c}_C$ at room temperature (Figure S26c, Supporting Information, 1:1, 5 mM), two different sets of resonances were observed, which are ascribed to a perched complex $\mathbf{1}\cdot\mathbf{2c}_C$ and an inclusion complex $\mathbf{1}\subset\mathbf{2c}_C$. This observation indicates that the two species interchange slowly on the ^{1}H NMR time scale. For the inclusion complex $\mathbf{1}\subset\mathbf{2c}_C$, a strong downfield shift ($\Delta\delta$ = 3.84 ppm) of the imide proton resonances compared with free thread **1** and downfield shifts ($\Delta\delta$ = 1.37 and 1.56 ppm) of the protons H_{NH1} and H_{NH2} compared with free receptor $\mathbf{2c}_C$ were observed, consistent with the findings from the ^{1}H NMR analysis of the [2]rotaxane $\mathbf{1}\subset\mathbf{2b}_C$. The different chemical shift values of the N−H resonances and pertinent aliphatic protons (H_A of the receptor part, H_a and H_g of the barbiturate part) of all the perched, interlocked, and inclusion complexes are summarized in Table 2.

A variable temperature ^{1}H NMR experiment on the perched complex with $\mathbf{1}\cdot\mathbf{2c}_C$ (Figure S27, Supporting Information, 1:1, 5 mM) was performed in $CDCl_3$ in the 0−55 °C range. Based on chemical shift changes and varying intensities of imide proton and receptor amide proton resonances, the kinetically labile nature of the inclusion complex $\mathbf{1}\subset\mathbf{2c}_C$ and the perched complex $\mathbf{1}\cdot\mathbf{2c}_C$ for thread **1** in the presence of a relatively large ring of receptor $\mathbf{2c}_C$ was evidenced. This is consistent with ring and stopper sizes estimated through molecular modeling (*vide supra*). In contrast, the kinetically inert nature of interlocked complex $\mathbf{1}\subset\mathbf{2b}_C$ was evidenced via slippage experiments (Figure S28, Supporting Information, 10 mM) in competitive DMSO solvent, due to the absence of dethreading, as judged by ^{1}H NMR spectroscopy, even upon heating $\mathbf{1}\subset\mathbf{2b}_C$ (10 mM) for several days at 80 °C (heating at this temperature provoked no retrodimerization of the HT photodimers). Similarly, an equimolar mixture of preformed macrocycle $\mathbf{2b}_C$ and **1** in noncompetitive $CDCl_3$ solvent was heated at 60 °C for several days and showed no evidence of threading (Figure S29, Supporting Information, 1:1, 5 mM). A slippage experiment between **1** and small macrocycle $\mathbf{2a}_C$ was also investigated in similar conditions (Figure S30, Supporting Information, 1:1, 5 mM) and showed no evidence for threading, conclusively demonstrating that [2]rotaxane formation by photocapture with the smallest receptor **2a**, unlike **2b** and **2c**, was not possible.

CONCLUSIONS

In summary, an unprecedented route for mechanically interlocked molecule (MIM) formation by photoclipping a synthetic receptor containing terminal anthracene groups onto a stoppered thread was developed. A barbiturate templating motif proved effective in preorganizing an acyclic Hamilton-type receptor using a six hydrogen-bond array with a high binding constant, without compromising the photochemical efficiency of the anthracene units, as shown by the unchanging photochemical quantum yields. A [2]rotaxane whose bead component was of intermediate ring size (36 members) proved optimal for photochemical MIM synthesis as indicated by NMR and molecular modeling. In contrast, a smaller homologous ring (30 members) proved too small, while a larger photomacrocycle (42 members) was able to undergo slippage over the *tert*-butyl decorated trityl stoppers. This behavior was rationalized using molecular modeling (PM6). Thermal reversion of the MIM and multicycle use of the system was demonstrated. Work is in progress to develop multistation H-bonding light-driven variants using these motifs.

EXPERIMENTAL SECTION

Synthesis. The molecular thread (**1**)[9] and receptors **2a**, **2b**, $\mathbf{2a}_C$, and $\mathbf{2b}_C$[10b] were previously reported.

Synthesis of Ethyl 10-(Anthracen-9-yloxy)decanoate (3). Acetone (200 mL) was added to a round-bottom flask and degassed for 30 min, before addition of anthrone (2.79 g, 14.4 mmol) and K_2CO_3 (1.98 g, 14.4 mmol). After the mixture was stirred for 10 min, the flask was heated to reflux at which point ethyl 10-bromodecanoate (4.00 g, 14.4 mmol) was added. The solution was maintained at reflux for 24 h. After cooling, the mixture was filtered, and the filtrate was evaporated to dryness. The resulting residue was dissolved in DCM (100 mL) and washed with water (50 mL). The organic phase was then dried using $MgSO_4$, filtered, and evaporated. The resulting orange oil was purified via column chromatography on silica (eluent, DCM/hexane (7/3, v/v)) to give 3.54 g of an orange oil. Yield: 62%. ^{1}H NMR (300 MHz, $CDCl_3$): δ 8.31−8.27 (m, 2H), 8.22 (s, 1H), 8.01−7.90 (m, 2H), 7.50−7.40 (m, 4H), 4.21−3.95 (m, 4H), 2.31 (t, J = 7.5 Hz, 2H), 2.00 (dd, J = 8.4, 6.8 Hz, 2H), 1.68−1.48 (m, 4H), 1.41−1.24 (m, 10H), 1.22 (t, J = 7.1 Hz, 3H). ^{13}C NMR (101 MHz, $CDCl_3$): δ 173.9, 151.5, 134.1, 132.4, 128.4, 127.2, 125.4, 125.0, 124.7, 122.4, 121.9, 76.2, 60.2, 34.4, 30.7, 29.5, 29.5, 29.3, 29.2, 26.2, 25.0, 14.3. HRMS (ES^+): calcd for $C_{26}H_{33}O_3$ m/z = 393.2424, found m/z = 393.2419. IR (neat): 3077 (CH) 2928 (CH) 2855 (CH) 1678 (CO).

Synthesis of 10-(Anthracen-9-yloxy)decanoic Acid (4). Ethyl 10-(anthracen-9-yloxy)decanoate (3.50 g, 8.9 mmol) was dissolved in a round-bottom flask containing ethanol (100 mL). A 10% NaOH solution (100 mL) was then added, and the mixture was heated under reflux for 14 h. Once the mixture was cooled to room temperature, the ethanol was removed under vacuum to afford a solid, which was then dissolved in water (400 mL). To this, conc. HCl was added dropwise with stirring to pH = 6, at which point an oily solid forms. The solid was dissolved in ethyl acetate, dried using $MgSO_4$, filtered, and evaporated to afford an orange solid (2.19 g). Yield: 67%. ^{1}H NMR (300 MHz, $CDCl_3$): δ 8.32−8.29 (m, 2H), 8.22 (s, 1H), 7.98 (m, 2H), 7.51−7.40 (m, 4H), 4.20 (t, J = 6.6 Hz, 2H), 2.38 (t, J = 7.4 Hz, 2H), 2.03 (dt, J = 12.8, 5.4 Hz, 2H), 1.69−1.60 (m, 4H), 1.56−1.30 (m,

dx.doi.org/10.1021/jo502452t | J. Org. Chem. 2015, 80, 988−996

8H). ^{13}C NMR (101 MHz, $CDCl_3$): δ 179.6, 151.5, 132.4, 128.4, 125.4, 125.0, 124.7, 122.5, 122.0, 76.2, 34.2, 30.7, 29.5, 29.5, 29.3, 29.1, 26.2, 24.8. HRMS (ES^+): calcd for $C_{24}H_{29}O_3$ m/z = 365.2117, found m/z = 365.2119. Mp: 208−210 °C. IR (neat): 3243 (OH) 2913 (CH) 2849 (CH) 1675 (CO).

Synthesis of 2,5-Dioxopyrrolidin-1-yl 10-(Anthracen-9-yloxy)decanoate (5). 10-(Anthracen-9-yloxy)decanoic acid (0.995 g, 2.70 mmol) and *N*-hydroxysuccinimide (0.311 g, 2.7 mmol) were dissolved in dry ethyl acetate (25 mL) in a round-bottom flask. A solution of *N*,*N*′-dicyclohexylcarbodiimide (0.613 g, 2.97 mmol) in ethyl acetate (15 mL) was then added dropwise via syringe, and the resulting solution was stirred at room temperature for 48 h. The suspension formed was filtered through a sintered funnel, and the filtrate was then concentrated under reduced pressure to form an orange oil. The flask was then cooled on ice for 4 h to form pure 2,5-dioxopyrrolidin-1-yl 10-(anthracen-9-yloxy)decanoate as a white/yellow precipitate (1.24 g), which was then dried under vacuum. Quantitative yield. ^{1}H NMR (400 MHz, $CDCl_3$): δ 8.31−8.21 (m, 2H), 8.21 (s, 1H), 8.00−7.98 (m, 2H), 7.50−7.44 (m, 4H), 4.20 (t, J = 6.6 Hz, 2H), 2.81 (s, 4H), 2.62 (t, J = 7.5 Hz, 2H), 2.09−2.02 (quin, J = 8.0 Hz, 2H), 1.77 (quin, J = 7.9 Hz, 2H), 1.75−1.64 (quin, J = 6.8 Hz, 2H), 1.49−1.30 (m, 8H). ^{13}C NMR (101 MHz, $CDCl_3$): δ 169.2, 168.7, 151.5, 132.4, 128.4, 125.5, 125.0, 124.7, 122.5, 121.9, 76.2, 31.0, 30.7, 29.5, 29.3, 29.1, 28.8, 26.2, 25.6, 24.6. HRMS (ES^+): calcd for $C_{28}H_{32}NO_5$ m/z = 462.2280, found m/z = 462.2276. Mp: 88−90 °C. IR (neat): 2924 (CH) 2849 (CH) 1778 (CO) 1731 (CO).

Synthesis of *N*-(6-Aminopyridin-2-yl)-10-(anthracen-9-yloxy)decanamide (6). Diisopropylethylamine (0.70 mL, 3.98 mmol) and an excess of 2,6-diaminopyridine (2.89 g, 26.5 mmol) were suspended in dry DCM (55 mL). A solution of 2,5-dioxopyrrolidin-1-yl 10-(anthracen-9-yloxy)decanoate (1.22 g, 2.65 mmol) in DCM (18 mL) was then added dropwise with stirring. The mixture was then heated to reflux for 5 days. Once cooled to room temperature, the suspension was filtered, and the filtrate washed with water (3 × 85 mL). The organic phase was then dried using $MgSO_4$, filtered, and evaporated. The crude oil obtained was purified via column chromatography on silica (eluent DCM/EtOAc (9/1, v/v)) to give 0.483 g of pure *N*-(6-aminopyridin-2-yl)-10-(anthracen-9-yloxy)-decanamide as a yellow solid. Yield: 40%. ^{1}H NMR (300 MHz, $CDCl_3$): δ 8.30−8.27 (m, 2H), 8.21 (s, 1H), 8.01−7.97 (m, 2H), 7.82 (s, 1H), 7.57 (d, J = 7.9 Hz, 1H), 7.55−7.40 (m, 5H), 6.22 (d, J = 8.7 Hz, 1H), 4.35 (s, 2H), 4.18 (t, J = 6.6 Hz, 2H), 2.36 (t, J = 7.5 Hz, 2H), 2.07−2.02 (m, 2H), 1.73−1.63 (m, 4H), 1.42−1.30 (m, 8H). ^{13}C NMR (101 MHz, $CDCl_3$): δ 171.6, 156.9, 151.5, 149.7, 140.3, 132.4, 128.4, 125.4, 125.0, 124.7, 122.5, 121.9, 104.2, 103.2, 76.2, 37.9, 30.7, 29.5, 29.5, 29.3, 29.2, 26.2, 25.4. HRMS (ES^+): cald. for $C_{29}H_{34}N_3O_2$ m/z = 456.2651, found m/z = 456.2643. Mp: 63−65 °C. IR (neat): 3336 (N−H) 2926 (C−H) 2853 (C−H) 1676 (CO) 1617 (CO).

Synthesis of Acyclic Receptor 2c. In a round-bottom flask, *N*-(6-aminopyridin-2-yl)-10-(anthracen-9-yloxy)decanamide (0.483 g, 1.1 mmol) and triethylamine (0.017 mL, 1.15 mmol) were dissolved in THF (65 mL). A solution of isophthaloyl chloride (0.125 g, 0.49 mmol) in THF (25 mL) was added dropwise at room temperature. A catalytic amount of DMAP was added to the flask, and the reaction mixture was left stirring for 48 h at 60 °C. After cooling, the suspension was filtered, and the solvent was removed under reduced pressure. The crude product was then purified via column chromatography on silica (eluent DCM/EtOAc, 85%/15% (v/v)) to give 0.284 g of pure acyclic receptor **2c** as a yellow solid. Yield: 53%. ^{1}H NMR (300 MHz, $CDCl_3$): δ 8.54 (s, NH), 8.22−8.14 (m, 4H), 8.09 (m, 3H), 8.01 (s, 2H), 7.95−7.82 (m, 9H), 7.62 (t, J = 8.1 Hz, 2H), 7.41−7.28 (m, 8H), 4.07 (t, J = 6.7 Hz, 4H), 2.28 (t, J = 7.5 Hz, 4H), 1.93 (p, J = 6.8 Hz, 4H), 1.57 (dq, J = 29.4, 7.2 Hz, 8H), 1.31−1.26 (m, 16H), 1.25 (s, 9H). ^{13}C NMR (101 MHz, $CDCl_3$): δ 172.0, 165.0, 153.3, 151.4, 149.9, 149.5, 140.9, 134.3, 132.4, 128.5, 128.4, 125.4, 125.0, 124.7, 122.6, 122.4, 122.0, 110.1, 109.7, 76.1, 37.7, 31.1, 30.7, 29.6, 29.5, 29.4, 29.2, 26.2, 25.4. HRMS (ES^+): cald. for $C_{70}H_{77}N_6O_6$ m/z = 1097.5905, found m/z = 1097.5913. Mp: 99−101 °C. IR (neat): 3283 (N−H) 3054 (N−H) 2926 (C−H) 2854 (C−H) 1678 (CO) 1584 (CO). UV−vis (CH_2Cl_2): 300 (24300); 352 (10400); 370 (15800); 391 (13650).

General Prodecure for the Synthesis of Macrocyclic Receptors $2c_C$. For large scale preparation, a solution of **2a**, **2b**, or **2c** in distilled dichloromethane at a concentration of 500 μM was irradiated with a Hanovia 450W HgXe lamp using a solution filter (lead nitrate/potassium bromide, 7g·L^{-1}; KBr 540 g·L^{-1}), which cut UV light below 350 nm. During the irradiation, a continuous bubbling of argon is necessary to avoid photo-oxidation. After 14 h of irradiation, the solvent was removed, and the residue was dissolved in THF, precipitated with hexane, and dried under vacuum. Characterization of $2a_C$ and $2b_C$ was reported previously.[10b]

$2c_C$. ^{1}H NMR (600 MHz, $CDCl_3$): δ 1.39−1.49 (m, 16H), 1.63 (s, 9H), 1.78 (m, 4H), 1.84 (m, 4H), 2.41 (t, J = 6.0 Hz, 4H), 3.51 (t, J = 6.0 Hz, 4H), 4.42 (s, 2H), 6.75−6.82 (m, 8H), 6.92−6.96 (m, 4H), 6.97−7.01 (m, 4H), 7.63 (s, 2H), 7.74 (t, J = 7.0 Hz, 2H), 7.99 (d, J = 6.0 Hz, 2H), 8.03 (d, J = 6.0 Hz, 2H), 8.12 (s, 2H), 8.21 (s, 1H), 8.30 (s, 2H). ^{13}C NMR (75 MHz, $CDCl_3$): δ 171.6, 164.9, 153.4, 149.6, 149.3, 142.1, 141.0, 140.9, 135.0, 127.9, 127.5, 125.7, 125.5, 125.0, 109.9, 109.7, 89.2, 64.9, 63.9, 38.0, 35.3, 31.2, 30.9, 30.0, 29.7, 29.0, 28.9, 28.8, 25.9, 25.4. HRMS (FD): cald for $C_{70}H_{76}N_6O_6$ m/z = 1096.58263; found m/z = 1096.58313. Mp: 125−128 °C. IR (neat): 3423 (N−H) 3064 (N−H) 2936 (C−H) 2857 (C−H) 1682 (CO) 1586 (CO). UV−vis (CH_2Cl_2): 299 (30150).

Procedure for the Synthesis of Rotaxanes via Dimerization of Acyclic Receptors: [2]Rotaxane ($1\subset 2b_C$). A solution of receptor (**2b**) in degassed DCM (25 mL) at c = 5 × 10^{-4} M, containing barbiturate thread **1** (3 equiv) was irradiated with a UV lamp using a band-pass filter at 365 nm. The dimerization was monitored using UV−vis absorption to observe the decrease in anthracene signal, and once complete, the solvent was removed, and the white solid obtained was purified via column chromatography (eluent DCM/ethyl acetate, 9/1, v/v) to give the rotaxane $1\subset 2b_C$ as a white solid. Yield 58%. ^{1}H NMR (300 MHz, acetone-d_6): δ 9.32 (NH, 2H), 8.15 (s, 1H), 8.06 (s, 2H), 7.89 (d, J = 7.2 Hz, 2H), 7.80 (d, J = 8.1 Hz, 2H), 7.68 (t, J = 8.1 Hz, 2H), 7.55 (s, 2H), 7.22−7.13 (m, 12H), 7.02−6.89 (m, 20H), 6.82−6.77 (m, 4H), 6.72−6.65 (m, 4H), 6.56 (pd, J = 7.4, 1.5 Hz, 8H), 4.95 (s, 4H), 4.40 (s, 2H), 3.75−3.59 (m, 8H), 2.33 (t, J = 7.6 Hz, 4H), 2.03−2.1 (m, 4H), 1.70−1.59 (m, 4H), 1.49−1.26 (m, 16H), 1.22 (s, 9H), 1.17 (s, 54H). ^{13}C NMR (126 MHz, acetone-d_6): δ 174.2, 172.5, 166.4, 157.3, 153.3, 151.8, 151.6, 151.1, 151.0, 149.2, 145.1, 144.4, 144.2, 141.4, 140.7, 135.5, 132.8, 131.4, 129.8, 128.0, 126.9, 126.2, 125.8, 125.0, 124.3, 123.6, 114.2, 111.3, 110.5, 90.3, 66.3, 63.9, 62.6, 62.4, 55.6, 49.8, 37.6, 36.0, 34.9, 31.7, 31.4, 31.4, 31.1, 30.0, 25.8. MS (ESI) cald for $C_{154}H_{172}N_{14}O_{11}$ m/z = 1197.2 $[M + 2H]^{2+}$, found m/z = 1197.3 $[M + 2H]^{2+}$. HRMS (FD) cald for $C_{154}H_{170}N_{14}O_{11}$ m/z = 2391.3174, found m/z = 2391.3153, cald for $C_{154}H_{170}N_{14}O_{11}Na$ m/z = 2414.3071, found m/z = 2414.3100. mp 156−158 °C. IR (KBr): 3434 (N−H) 2924 (C−H) 2854 (C−H) 1637 (CO) 1505 (CO). UV−vis (CH_2Cl_2): 299 (34500).

■ ASSOCIATED CONTENT

Supporting Information

^{1}H, ^{13}C, and HRMS spectra of compounds **2c**, $2c_C$, **3**, **4**, **5**, **6**, and $1\subset 2b_C$, 2D NMR investigation of $1\subset 2b_C$ (ROESY and DOSY NMR), photochemical and molecular modeling methods, calculated structure of $1\subset 2a_C$ and $1\subset 2c_C$, and electronic absorption and fluorescence spectra. This material is available free of charge via the Internet at http://pubs.acs.org.

■ AUTHOR INFORMATION

Corresponding Authors

*E-mail: nathan.mcclenaghan@u-bordeaux.fr (N.McC.).
*E-mail: j.tucker@bham.ac.uk (J.H.R.T.).

Notes

The authors declare no competing financial interest.

■ ACKNOWLEDGMENTS

Financial support from the School of Chemistry at the University of Birmingham (Ph.D. studentships to P.J.T.), Advantage West Midlands for equipment, the EPSRC for the award of a Leadership Fellowship, Région Aquitaine, University of Bordeaux, CNRS, and Ministère de la Recherche et de l'Enseignement Supérieur (A.T.) are gratefully acknowledged.

■ REFERENCES

(1) (a) Reuter, C.; Seel, C.; Nieger, M.; Vögtle, F. *Helv. Chim. Acta* **2000**, *83*, 630. (b) Kay, E. R.; Leigh, D. A. *Top. Curr. Chem.* **2005**, *262*, 133. (c) Stoddart, J. F. *Chem. Soc. Rev.* **2009**, *38*, 1521. (d) Forgan, R. S.; Sauvage, J.-P.; Stoddart, J. F. *Chem. Rev.* **2011**, *111*, 5434. (e) Langton, M. J.; Matichak, J. D.; Thompson, A. L.; Anderson, H. L. *Chem. Sci.* **2011**, *2*, 1897. (f) Noujeim, N.; Zhu, K.; Vukotic, V. N.; Loeb, S. J. *Org. Lett.* **2012**, *14*, 2484. (g) Coskun, A.; Banaszak, M.; Astumian, R. D.; Stoddart, J. F.; Grzybowski, B. A. *Chem. Soc. Rev.* **2012**, *41*, 19. (h) Lewandowski, B.; De Bo, G.; Ward, J. W.; Papmeyer, M.; Kuschel, S.; Aldegunde, M. J.; Gramlich, P. M. E.; Heckmann, D.; Goldup, S. M.; D'Souza, D. M.; Fernandes, A. E.; Leigh, D. A. *Science* **2013**, *339*, 189. (i) Bordoli, R. J.; Goldup, S. M. *J. Am. Chem. Soc.* **2014**, *136*, 4817.

(2) (a) Leigh, D. A.; Lusby, P. J.; McBurney, R. T.; Morelli, A.; Slawin, A. M. Z.; Thomson, A. R.; Walker, D. B. *J. Am. Chem. Soc.* **2009**, *131*, 3762. (b) Guo, J.; Mayers, P. C.; Breault, G. A.; Hunter, C. A. *Nat. Chem.* **2010**, *2*, 218. (c) Clark, P. G.; Guidry, E. N.; Chan, W. Y.; Steinmetz, W. E.; Grubbs, R. H. *J. Am. Chem. Soc.* **2010**, *132*, 3405.

(3) (a) Hänni, K. D.; Leigh, D. A. *Chem. Soc. Rev.* **2010**, *39*, 1240. (b) Winn, J.; Pinczewska, A.; Goldup, S. M. *J. Am. Chem. Soc.* **2013**, *135*, 13318.

(4) (a) Yamashita, K.-I.; Kawano, M.; Fujita, M. *J. Am. Chem. Soc.* **2007**, *129*, 1850. (b) Zhou, W.; Zheng, H.; Li, Y.; Liu, H.; Li, Y. *Org. Lett.* **2010**, *12*, 4078. (c) Zheng, H.; Li, Y.; Zhou, C.; Li, Y.; Yang, W.; Zhou, W.; Zuo, Z.; Liu, H. *Chem.—Eur. J.* **2011**, *17*, 2160.

(5) Desvergne, J.-P.; Bouas-Laurent, H. *J. Chem. Soc., Chem. Commun.* **1978**, 403.

(6) (a) Desvergne, J.-P.; Bitit, N.; Castellan, A.; Webb, M.; Bouas-Laurent, H. *J. Chem. Soc., Perkin Trans. 2* **1988**, 1885. (b) McSkimming, G.; Tucker, J. H. R.; Bouas-Laurent, H.; Desvergne, J.-P.; Coles, S. J.; Hursthouse, M. B.; Light, M. E. *Chem.—Eur. J.* **2002**, *8*, 3331. (c) Dacarro, G.; Ricci, P.; Sacchi, D.; Taglietti, A. *Eur. J. Inorg. Chem.* **2011**, 1212.

(7) Hirose, K.; Shiba, Y.; Ishibashi, K.; Doi, Y.; Tobe, Y. *Chem.—Eur. J.* **2008**, *14*, 981.

(8) (a) Okada, M.; Takashima, Y.; Harada, A. *Macromolecules* **2004**, *37*, 7075. (b) Okada, M.; Harada, A. *Macromolecules* **2003**, *36*, 9701.

(9) Tron, A.; Thornton, P. J.; Rocher, M.; Jacquot de Rouville, H.-P.; Desvergne, J.-P.; Kauffmann, B.; Buffeteau, T.; Cavagnat, D.; Tucker, J. H. R.; McClenaghan, N. D. *Org. Lett.* **2014**, *16*, 1358.

(10) (a) Molard, Y.; Bassani, D. M.; Desvergne, J.-P.; Horton, P. N.; Hursthouse, M. B.; Tucker, J. H. R. *Angew. Chem., Int. Ed.* **2005**, *44*, 1072. (b) Molard, Y.; Bassani, D. M.; Desvergne, J.-P.; Moran, N.; Tucker, J. H. R. *J. Org. Chem.* **2006**, *71*, 8523.

(11) (a) Bouas-Laurent, H.; Castellan, A.; Desvergne, J.-P.; Lapouyade, R. *Chem. Soc. Rev.* **2000**, *29*, 43. (b) Bouas-Laurent, H.; Castellan, A.; Desvergne, J.-P.; Lapouyade, R. *Chem. Soc. Rev.* **2001**, *30*, 248.

(12) Schönberg, A. *Preparative Organic Photochemistry*; Springer-Verlag: Berlin, 1968; p 492.

(13) Eaton, D. E. *Handbook of Organic Photochemistry*; Scaiano, J. C., Ed.; CRC: Boca Raton, FL, 1989; Vol *1*.

(14) Desvergne, J.-P.; Bouas-Laurent, H. *Isr. J. Chem.* **1979**, *18*, 220.

(15) Montalti, M.; Credi, A.; Prodi, L.; Gandolfi, M. T. In *Handbook of Photochemistry*, 3rd ed.; CRC Press: New York, 2006; pp 601−604.